Electronic Supplementary Information

Synthesis, characterization and visible-light photocatalytic activity of

## Bi$_{24}$Al$_2$O$_{39}$ mesoporous hollow spheres

Zhen Wan[a], Gaoke Zhang[*a], Junting Wang[a], Yalei Zhang[*b]

a. School of Resources and Environmental Engineering, Wuhan University of
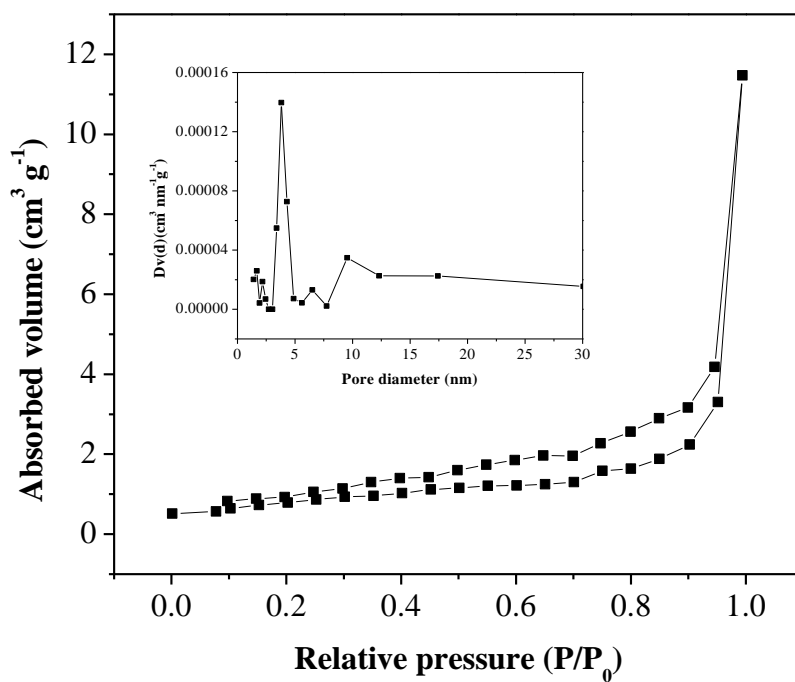
Technology, Wuhan, 430070, China

b. State Key Laboratory of Pollution Control and Resource Reuse, College of

Environmental Science and Engineering, Tongji University, Shanghai 200092, China

*Corresponding author. Tel: 86-27-87651816; fax: 86-27-87887445.

E-mail: gkzhang@whut.edu.cn; zhangyalei06@126.com.
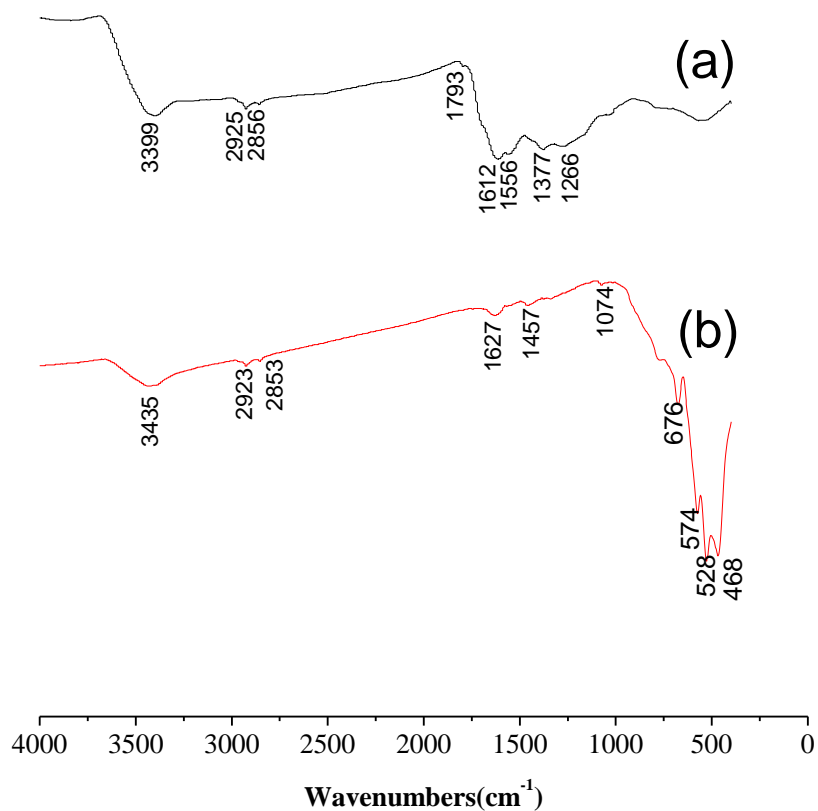
**Fig. S1** FR-IR spectra of (a) the BAO-20, (b) the BAO-20-550.

Fig. S2 N_2 adsorption-desorption isotherm of the BAO-20-550 catalyst. The insert is
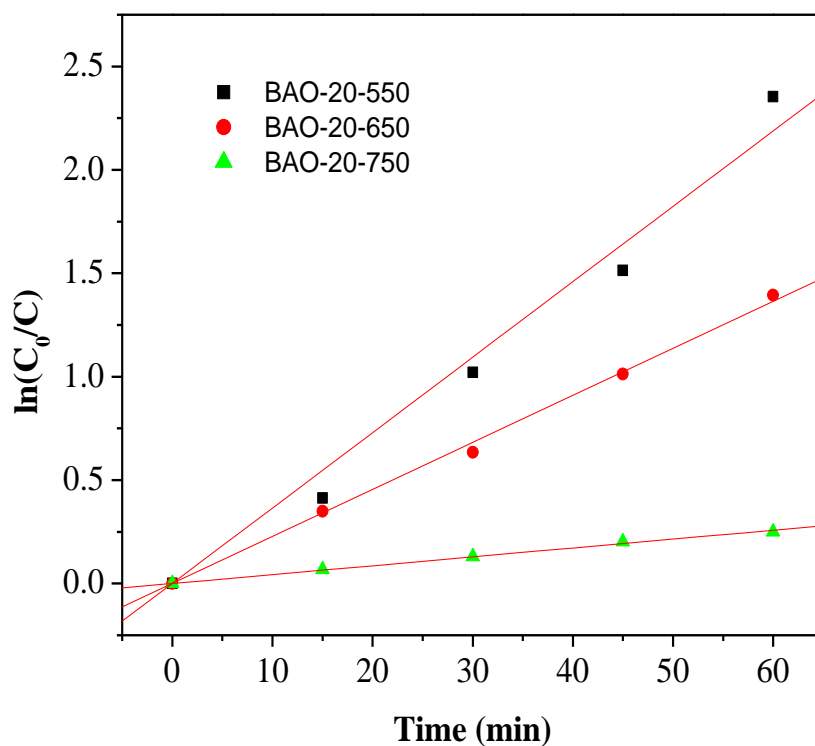
pore size distribution of the BAO-20-550 catalyst.

Table S1 BET surface area, pore volume and average pore size of the samples

| Samples	BAO-20-550	BAO-20-650	BAO-20-750	BAO-SSR
S_{BET} (m^2/g)	2.99	2.41	2.08	1.50
D_P (nm)	23.78	16.09	12.99	/^{a}
V_P (10^{-3} cm^3/g)	17.79	9.71	6.74	/^{a}

^{a} Too small to be detected.
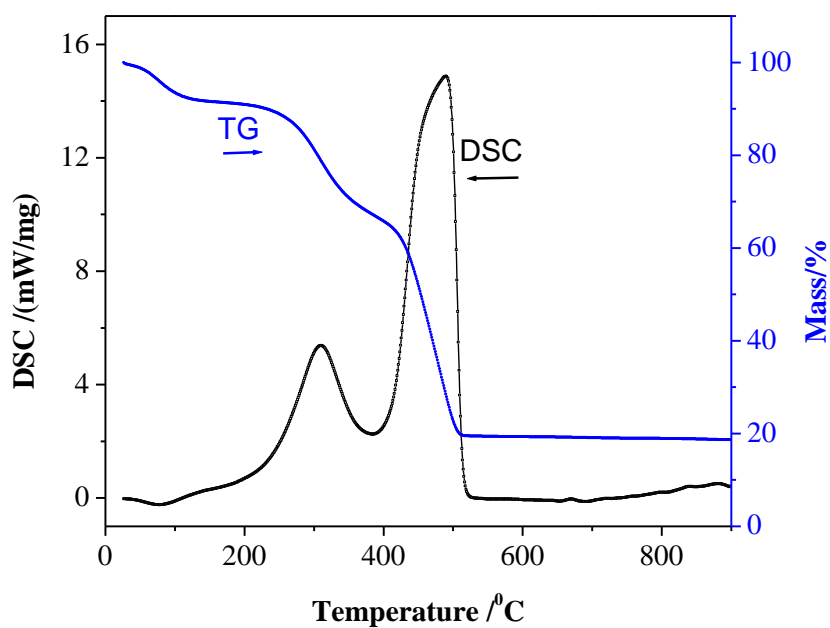
Fig. S3 TG-DSC curves of the uncalcinated sample.

Fig. S4 Kinetic studies for the degradation of ARG over the $Bi_{24}Al_2O_{39}$ mesoporous

hollow spheres obtained at different calcination temperature.

Table S2 Comparison of the kinetic parameters for the catalysts

Sample	Fitted equation	R	Rate constant k
BAO-20-550	$In(C_0/C) = 0.0365t$	0.9927	0.0365
BAO-20-650	$In(C_0/C) = 0.0227t$	0.9987	0.0227
BAO-20-750	$In(C_0/C) = 0.0043t$	0.9984	0.0043
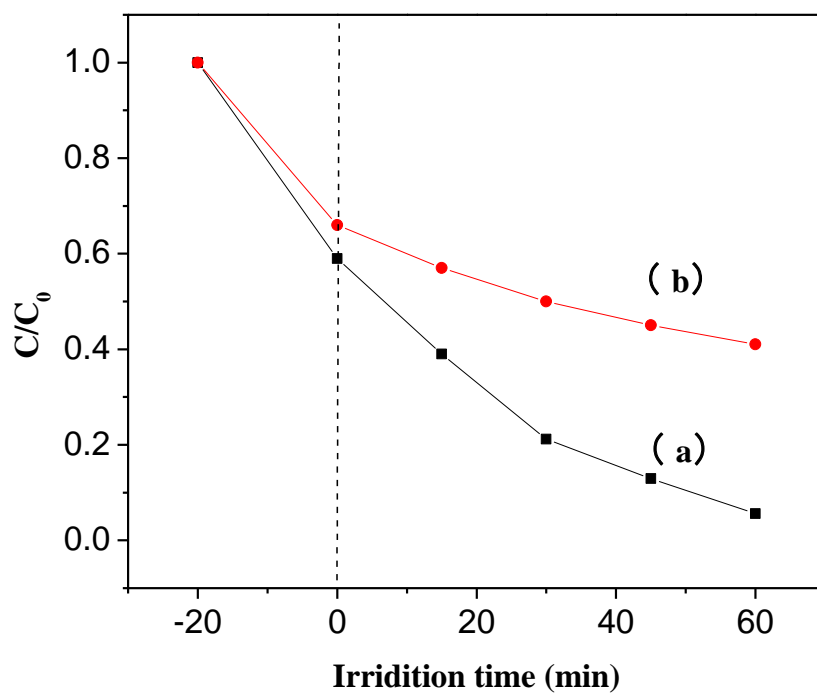
Fig. S5 Time-dependent photocatalytic degradation efficiency of ARG by (a) the

BAO-20-550, (b) the crushed BAO-20-550.
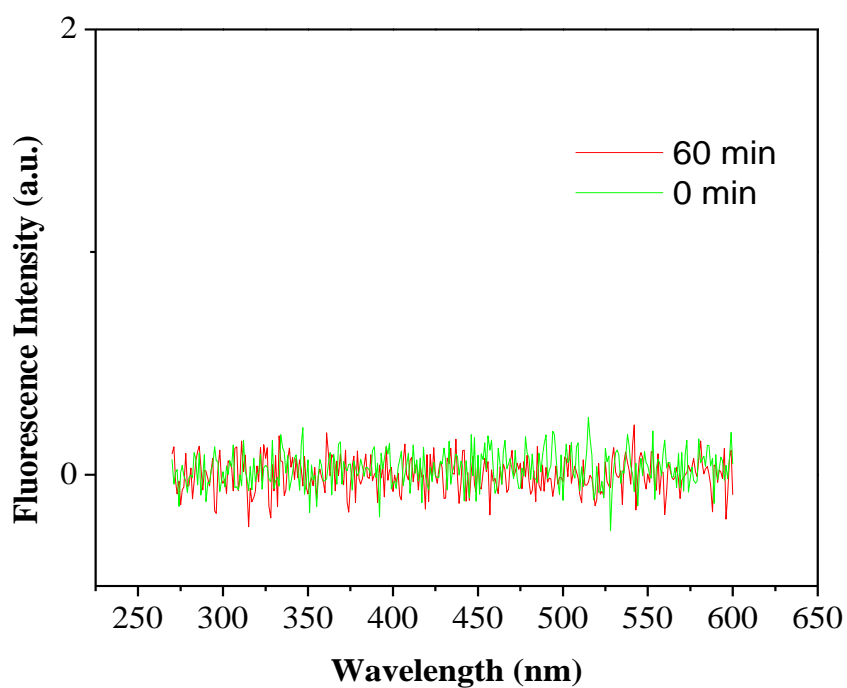
Fig. S6 $^{\cdot}$OH trapping photoluminescence spectra of the $Bi_{24}Al_2O_{39}$–TA suspension

under visible-light irradiation.